NASA TECHNICAL NOTE

NASA TN D-3685

NASA TN D-3685

AN INTEGRATED APPROACH TO THE ANALYSIS AND DESIGN OF WINGS AND WING-BODY COMBINATIONS IN SUPERSONIC FLOW

by Ralph L. Carmichael and Frank A. Woodward

Ames Research Center
Moffett Field, Calif.

NATIONAL AERONAUTICS AND SPACE ADMINISTRATION • WASHINGTON, D. C. • OCTOBER 1966

NASA TN D-3685

AN INTEGRATED APPROACH TO THE ANALYSIS AND DESIGN OF WINGS AND WING-BODY COMBINATIONS IN SUPERSONIC FLOW

By Ralph L. Carmichael and Frank A. Woodward

Ames Research Center
Moffett Field, Calif.

NATIONAL AERONAUTICS AND SPACE ADMINISTRATION

For sale by the Clearinghouse for Federal Scientific and Technical Information
Springfield, Virginia 22151 – Price $1.00

AN INTEGRATED APPROACH TO THE ANALYSIS AND DESIGN OF WINGS AND WING-BODY COMBINATIONS IN SUPERSONIC FLOW[1]

By Ralph L. Carmichael and Frank A. Woodward[2]
Ames Research Center

SUMMARY

A numerical procedure has been developed for analyzing wings and wing-body combinations and for designing optimum wing camber surfaces in the presence of a body. The method is very general and applies to wings of arbitrary planform and bodies of arbitrary cross section and camber. The procedure has been programmed for automatic computation and considerable effort has been made to allow the user to analyze a great variety of configurations with relatively simple input data.

For a given wing or wing-body combination, five classes of problems may be solved:

(1) Wing warp required to support a given loading on the wing

(2) Wing loading for a given wing warp

(3) Pressures on the upper and lower surfaces of a warped wing of small but finite thickness

(4) Minimum drag wing shape for a given lift constraint

(5) Minimum drag wing shape for a given lift and moment constraint

The validity of the method has been confirmed by comparison with exact solutions to the linearized flow equation for several simple wings and wing-body combinations. In addition theoretical and experimental results have been compared for more complex configurations.

INTRODUCTION

The work described in this paper has been undertaken in an effort to develop a procedure for designing wing-body combinations with low drag at supersonic speeds.

Several methods have been published which enable one to compute the camber surface of minimum drag for an isolated wing at a given lift. None

---

[1]Presented at NASA Conference on Aircraft Aerodynamics, Langley Research Center, May 23-25, 1966.

[2]The Boeing Company.

of these methods, however, considers the effect of the flow disturbance generated by the body on the shape of the optimum camber surface. The new method used in this work enables one to determine the lifting surface of minimum drag for a given value of lift in the presence of a body which may be at incidence relative to the free stream. In addition to this computation, the lift and drag of a configuration of given geometry may be determined, thereby providing the wing-body interference for configurations of arbitrary planform and camber. By using this procedure, one can assess the effects of such modifications as wing and body camber and incidence on the lift, drag, and moment characteristics of a given wing-body configuration.

The numerical procedure has been programed for automated computation for a great variety of configurations.

The theoretical analysis and the computer program used for the numerical computations in this paper were developed by the Aerodynamic Research Unit of the Airplane Group of The Boeing Company under NASA contract NAS2-2282. (See refs. 1 and 2.)

SYMBOLS

AR	aspect ratio
b	span
c	chord
C_{L_α}	slope of lift curve, $dC_L/d\alpha$, per radian
C_L	lift coefficient
C_m	pitching-moment coefficient
C_{m_o}	pitching moment at zero lift
ΔC_p	difference in pressure coefficient between upper and lower surfaces of wing
d	body diameter
L/D	lift-drag ratio
M	Mach number
P	difference between pressure coefficient at given angle of attack and pressure coefficient at zero angle of attack

r body radius

U_∞ free-stream velocity

x,y,z Cartesian coordinates

x' distance from the leading edge

α angle of attack

$\beta = \sqrt{M^2 - 1}$

Λ leading-edge sweep angle

METHOD OF ANALYSIS

The actual wing-body combination is replaced by distributions of singularities, which satisfy the linearized equation of supersonic flow, whose strengths are adjusted to satisfy the boundary conditions required by the geometry of the particular configuration. The wing warp and incidence are represented by distributions of vorticity corresponding to pressure differences across the wing. The wing thickness effect is given by sources and sinks located over the wing reference plane. The body thickness, camber, and incidence are simulated by line sources and doublets placed along the body reference axis. Finally, the interference effects of the wing on the body are cancelled by a distribution of vorticity on the surface of the body.

A typical wing-body combination is represented in figure 1. A grid which conforms to the general geometry of the configuration subdivides the wing and body into a large number of small panels. Each panel is a region over which a particular singularity strength is held constant. In this way, the continuous distribution of singularities representing the actual wing and body is approximated by simple functions with a finite range of values. Associated with each panel is a control point for matching the boundary conditions. At each control point, the flow must be tangential to the panel surface. In contrast to the wing-alone programs in common use which usually match only the downwash, the normal vector to the panel surface is used in this computation. The resultant normal velocity at each panel control point may now be expressed as a system of linear equations in terms of the singularity strengths. The coefficients of this system of equations are computed and stored as a matrix of aerodynamic influence coefficients. Then, for a given camber shape or pressure distribution, the various singularity strengths which satisfy all the boundary conditions are computed, and from these, the pressure distribution, lift, drag, and moment on the wing and body may be computed.

This method may be referred to as a near-field theory in that the forces are computed by integration of the local pressures over the surface of the

configuration. Of course, the results of a near- and a far-field theory will be identical except for the leading-edge suction force (on subsonic leading edges) which is not included in the surface-integration method.

Since the lift and drag of the configuration are functions of a finite number of real variables, the determination of the surface of minimum drag for a given lift constraint can now be solved by the Lagrange multiplier method.

A complete description of the theory and programing details is contained in references 1 and 2.

RESULTS AND DISCUSSION

Pressures and Forces on Flat Wings

The accuracy of the technique for computing pressures and forces on isolated wings is indicated in figures 2, 3, and 4. In each case, planforms have been selected for which exact solutions are known to the linearized equation of supersonic flow.

In figure 2, the program results are compared with exact conical flow theory for delta wings. Examples are shown for both subsonic and supersonic leading-edge wings. The symbols represent the pressures given by the program for wing chords located at 15, 45, and 75 percent of the semispan. The solid curves were computed from conical flow theory and may be found as solutions 3 and 6 in reference 3. The results agree quite well except at the sharp ridges of the supersonic solution. This rounding of the pressures computed by this program occurs because the pressures shown are actually average pressures over a wing panel.

The next example, illustrated in figure 3, is a test of the ability of the method to predict tip effect and to account for a subsonic trailing edge. The planform is a constant chord wing with $\beta AR = 1.92$. The leading and trailing edges are subsonic with $\beta \cot \Lambda = 0.6$. The program results along four different wing chords at 25, 50, 75, and 95 percent of the semispan are given by the symbols. The solid lines are the results given in reference 4 which were computed by the technique of superposing conical flows. As in the previous example, the program results agree very well except in the regions where the pressure distributions vary rapidly. Along the chords where the analytic solution varies rapidly, the program results underpredict the pressures in front of a sharp pressure drop and overpredict those behind the drop with the result that the integrated loadings are quite close to those of the analytic solution. This can be seen by the results shown in figure 4. The integrated loadings for a delta wing with 60° of leading-edge sweep are shown by the symbols. The solid curve is the well-known exact conical flow solution for a delta wing.

Wing-Body Loadings

To confirm the accuracy of the method for calculating wing-body interference, a configuration whose loading has been measured was studied. A sketch of the configuration is presented as figure 5. The rectangular wing of aspect ratio 3 is mounted in the midwing position on a cylindrical body with an ogival nose. The wind-tunnel model was constructed with pressure taps along 0° and 45° meridian lines on the body and along several chords on the wing. The pressures measured at a Mach number of 1.48 and reported in reference 5 are compared with the program results in figure 6. The parameter P represents the value of pressure coefficient at angle of attack less the pressure coefficient at zero angle of attack. The predicted pressures agree quite well with those measured experimentally at $\alpha = 2^\circ$. As the angle of attack increased, the agreement was less satisfactory.

The examples shown and other test cases studied provide confidence in the ability of the method to predict loadings, forces, and moments to a degree of accuracy well within the requirements of engineering design.

Prediction of the Effect of Wing and Body Camber

All the preceding results are accessible by established methods and serve to provide confidence in the method. The results to be shown in this section are not within the scope of any of the well-known methods.

The aerodynamic characteristics of a wing-body combination are sensitive to modifications, such as wing incidence relative to the body, wing or body camber, etc. In fact, it is precisely through modifications such as these that the characteristics of an airplane are brought in line with the design requirements. This computational method enables the designer to make accurate estimates of the effect of these changes to the basic configurations.

As reported in reference 6, a study was made of a series of wing-body wind-tunnel models employing various combinations of wing and body warps. The wing was arrow shaped with a leading-edge sweep angle of 70° and an aspect ratio of 2.24. Configuration 1 consisted of a flat wing on the uncambered body. Configuration 2 was made up of a cambered wing mounted on the uncambered body such that the body axis was at zero incidence when the wing was at the design condition; namely, $C_L = 0.08$ and $M = 2$. Configuration 3 had the same cambered wing but the axis of the body was alined with the root chord of the wing; also, the nose of the body was drooped and the rear portion of the body was swept upward.

The effects of these variations in model geometry are illustrated in figure 7. The symbols represent the experimental data reported in reference 6 and the curves are the program results. Since the theoretical method described in this paper does not include viscous effects, it was necessary to estimate the skin-friction drag in order to compare theoretical and experimental drag values. For this study, the skin friction was taken to be the difference between the experimental drag and the theoretical wave drag of the symmetrical

configuration at zero lift. This drag increment was then added to all the theoretical results to obtain the curves of theoretical lift-drag ratio as a function of lift coefficient. As predicted theoretically, none of the modifications changed the slope of the lift or moment curves. However, there were significant differences in the angle of attack at zero lift, pitching moment at zero lift, and maximum lift-drag ratio of the three configurations. As can be seen in figure 7, this method provides very accurate estimates of these quantities.

The characteristics of these wing-body combinations are somewhat different from those of the isolated wing, as can be seen in figure 8. The wing referred to in this figure is the cambered and twisted wing of reference 7 used in configurations 2 and 3 and the wing-body is configuration 2 of figure 7. One may observe that the wing alone has a C_{m_o} of approximately 0.01, whereas the body in combination with this wing has virtually no pitching moment at zero lift. In a similar manner, the lift curves of the two configurations are displaced. This indicates the importance of the body on the overall properties of wing-body combinations and may help to explain some of the discrepancies which have occurred between theory and experiment on wing-body combinations designed by wing-alone computing programs.

Effect of Body Size on Shape of the Minimum Drag Wing

One of the unique features of this computing procedure is the ability to compute the surface of minimum drag for a given wing planform in the presence of a body which may be at incidence relative to the wind. To illustrate the importance of the body flow field a study has been made of the minimum drag shape of a given wing with different size bodies. The basic wing planform is a simple delta wing with $\beta \cot \Lambda = 0.3$ which corresponds to a leading-edge sweep of 73.3° at a Mach number of $\sqrt{2}$. The shape of the isolated wing with minimum drag for a fixed lift is illustrated in figure 9. Five sections are shown through this wing constructed with the leading edge in the x-y plane. The straight reference lines are the intersection of the section plane with the x-y plane. The same wing was then analyzed in combination with bodies of various sizes, one of which is shown in figure 10. The shape of the wing in the presence of this small body is similar to the shape of the isolated wing. This confirms the intuitive conclusion that a small body should have a small effect on the optimum wing shape. As the ratio of body diameter to wing span was increased, the shape of the minimum drag camber surface for the wing-body combination varied considerably from the shapes shown in figures 9 and 10. The effect on this shape of such variables as nose length and shape, incidence of the body relative to the free stream, and location of the wing on the body has not been adequately investigated at this time. For this reason, the shapes of these wings are not presented.

The theoretical model upon which these calculations are based assumes inviscid flow. For this reason, these shapes should be viewed cautiously as far as actual experimental performance is concerned.

CONCLUDING REMARKS

The computational method whose results are described in this paper provides the designer with the ability to predict the longitudinal characteristics of wing-body combinations of arbitrary planform, camber, twist, and thickness. By this procedure one may accurately estimate many important performance parameters which are not available by the older techniques now in use. The technique is rapid and straightforward enough to be used in engineering design studies of families of configurations. The program is written for the class of computers in wide use by the aviation industry today. With the optimization capability built into the program it should be possible to calculate low-drag wing-body combinations to be used as the basis for designing efficient aerodynamic vehicles.

Ames Research Center
National Aeronautics and Space Administration
Moffett Field, Calif., May 23, 1966
126-13-02-12

REFERENCES

1. Woodward, F. A.; and Larson, J. W.: A Method of Optimizing Camber Surfaces for Wing-Body Combinations at Supersonic Speeds. Part I - Theory and Application. Doc. D6-10741, Pt. I, The Boeing Co., 1965. (Prepared for NASA under contract NAS2-2282.)

2. Brown, J. E.; Kawaguchi, A. S.; and LaRowe, Eugene: A Method of Optimizing Camber Surfaces for Wing-Body Combinations at Supersonic Speeds. Part II - Digital Computer Program Description. Doc. D6-10741, Pt. II, The Boeing Co., 1965. (Prepared for NASA under contract NAS2-2282.)

3. Jones, Robert T.; and Cohen, Doris: High Speed Wing Theory. Princeton Univ. Press, 1960, pp. 156-157.

4. Cohen, Doris: Formulas for the Supersonic Loading, Lift and Drag of Flat Swept-Back Wings With Leading Edges Behind the Mach Lines. NACA Rept. 1050, 1951.

5. Nielsen, Jack N.: Quasi-Cylindrical Theory of Wing-Body Interference at Supersonic Speeds and Comparison With Experiment. NACA Rept. 1252, 1955. (Supersedes NACA TN 2677 by Nielsen and Pitts and NACA TN 3128 by Pitts, Nielsen, and Gionfriddo.)

6. Carlson, Harry W.: Longitudinal Aerodynamic Characteristics at Mach Number 2.02 of a Series of Wing-Body Configurations Employing a Cambered and Twisted Arrow Wing. NASA TM X-838, 1963.

7. Carlson, Harry W.: Aerodynamic Characteristics at Mach Number 2.05 of a Series of Highly Swept Arrow Wings Employing Various Degrees of Twist and Camber. NASA TM X-332, 1960.

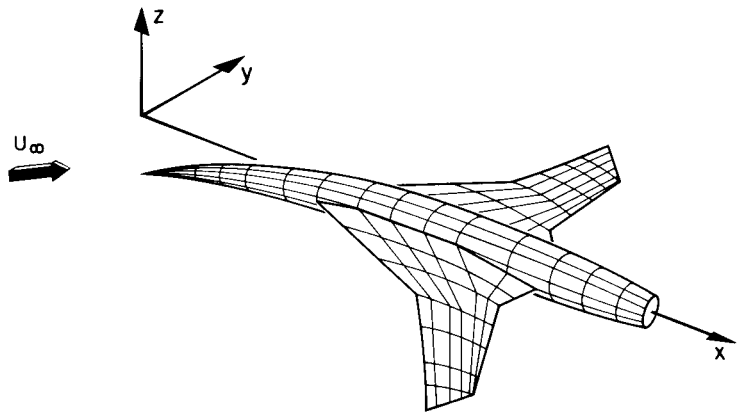

Figure 1.- Typical panel layout for wing-body combination.

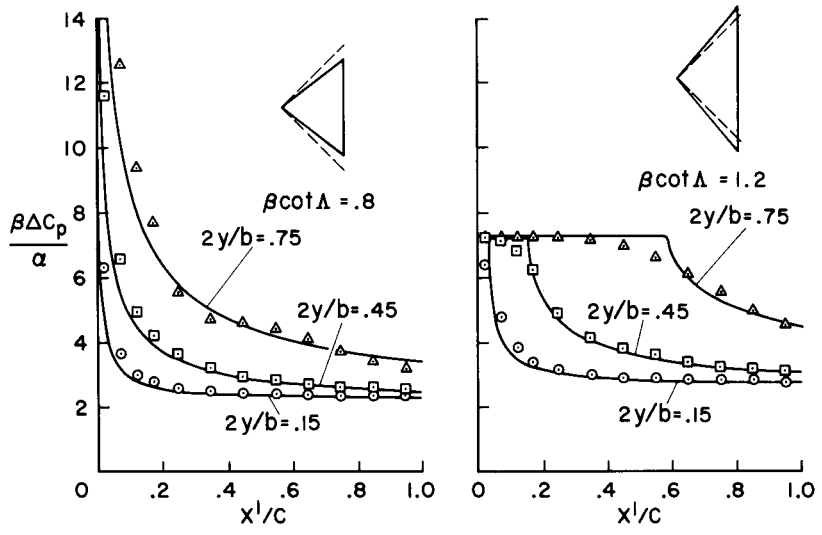

Figure 2.- Comparison between exact linear theory and program results for delta wings.

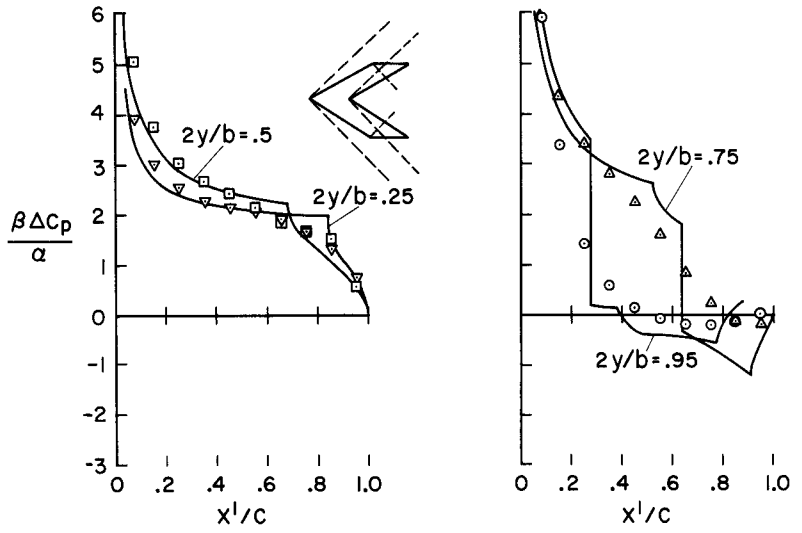

Figure 3.- Comparison between exact linear theory and program results for a swept wing.

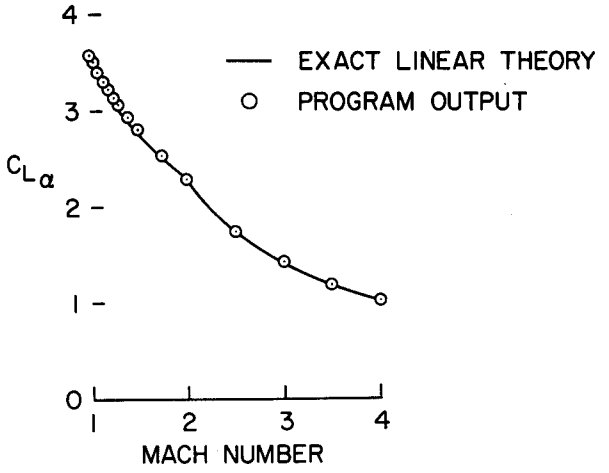

Figure 4.- Lift curve slope of delta wing, $\Lambda = 60^\circ$.

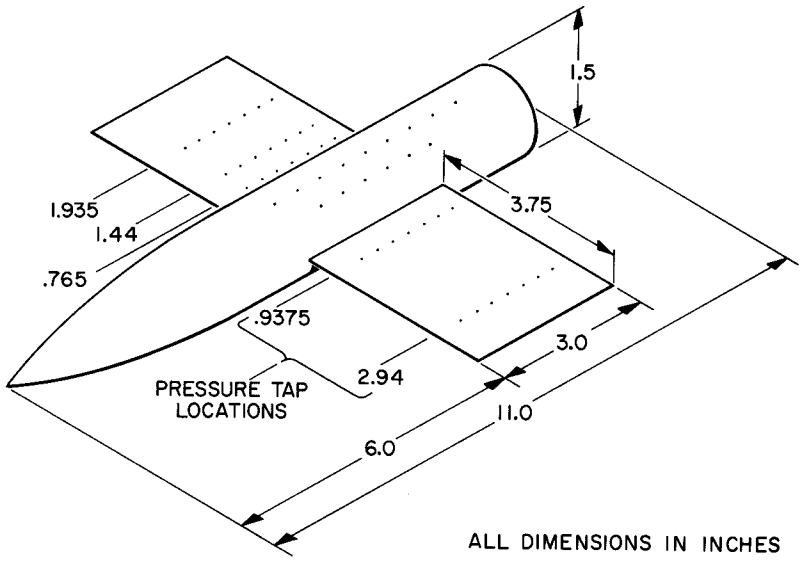

Figure 5.- Wing-body pressure model.

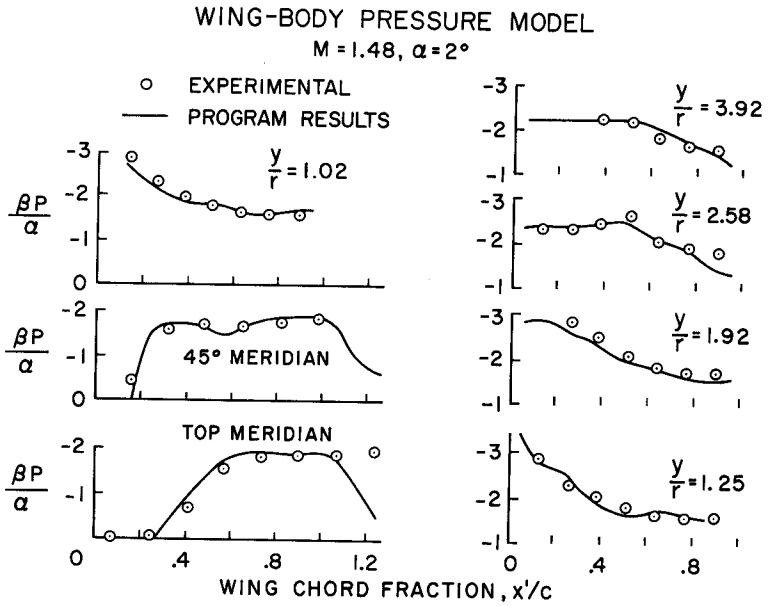

Figure 6.- Wing-body pressure model.

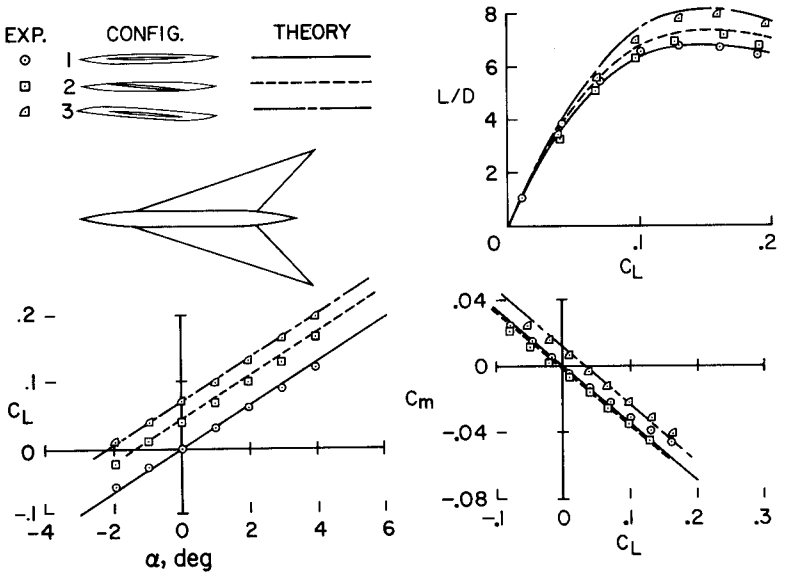

Figure 7.- Effect of wing and body camber at M = 2.

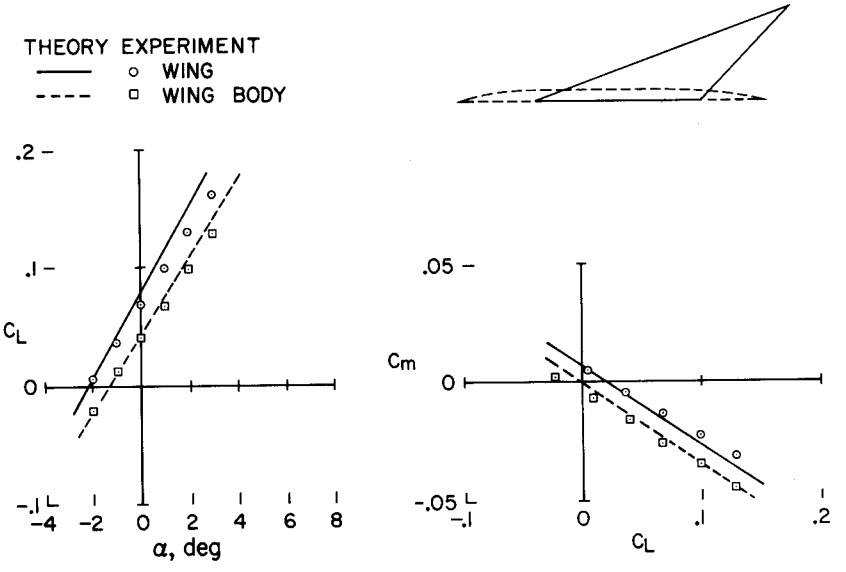

Figure 8.- Wing alone and wing-body characteristics at M = 2.

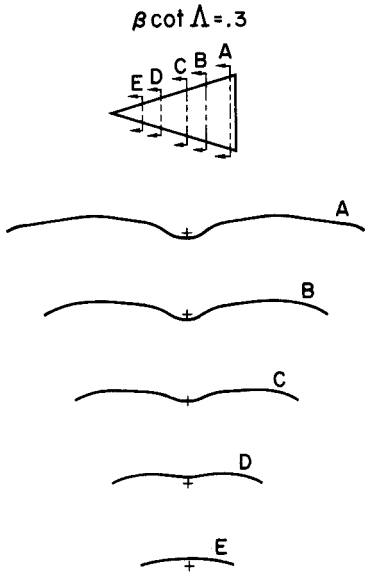

Figure 9.- Wing alone optimum camber surface.

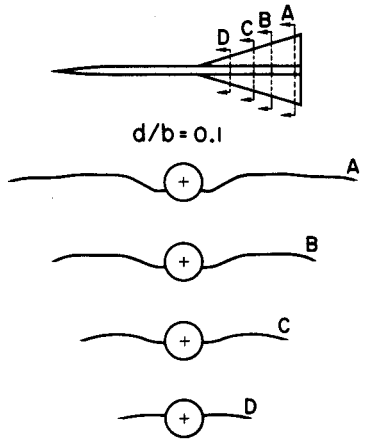

Figure 10.- Effect of body on optimum camber surface.